Heat shock protein expression as guidance for the therapeutic window of retinal laser therapy

Jenny Wang[*a], Philip Huie[b,c], Roopa Dalal[b], Seungjun Lee[d], Gavin Tan[e], Daeyoung Lee[f], Daniel Lavinksy[g], Daniel Palanker[a,b]

[a]Department of Applied Physics, Stanford University, CA, USA, 94025; [b]Department of Opthalmology, Stanford University, CA, USA, 94025; [c]Hansen Experimental Physics Laboratory, Stanford University, CA, USA, 94025; [d]Department of Ophthalmology, Kangwon National University, Chuncheon, South Korea; [e]Singapore National Eye Centre, Singapore; [f]Department of Ophthalmology, Gachon University Gil Medical Center, Incheon, South Korea; [g]Department of Ophthalmology, Federal University Rio Grande do Sul, Porto Alegre, Brazil

ABSTRACT

Unlike conventional photocoagulation, non-damaging retinal laser therapy (NRT) limits laser-induced heating to stay below the retinal damage threshold and therefore requires careful dosimetry. Without the adverse effects associated with photocoagulation, NRT can be applied to critical areas of the retina and repeatedly to manage chronic disorders. Although the clinical benefits of NRT have been demonstrated, the mechanism of therapeutic effect and width of the therapeutic window below damage threshold are not well understood. Here, we measure activation of heat shock response via laser-induced hyperthermia as one indication of cellular response. A 577 nm laser is used with the Endpoint Management (EpM) user interface, a titration algorithm, to set experimental pulse energies relative to a barely visible titration lesion. Live/dead staining and histology show that the retinal damage threshold in rabbits is at 40% of titration energy on EpM scale. Heat shock protein 70 (HSP70) expression in the retinal pigment epithelium (RPE) was detected by whole-mount immunohistochemistry after different levels of laser treatment. We show HSP70 expression in the RPE beginning at 25% of titration energy indicating that there is a window for NRT between 25% and 40% with activation of the heat shock protein expression in response to hyperthermia. HSP70 expression is also seen at the perimeter of damaging lesions, as expected based on a computational model of laser heating. Expression area for each pulse energy setting varied between laser spots due to pigmentation changes, indicating the relatively narrow window of non-damaging activation and highlighting the importance of proper titration.

Keywords: retina, laser therapy, non-damaging, hyperthermia, heat shock protein, retinal pigment epithelium

*email: jywang2@stanford.edu; phone: (631)-974-4986

1. INTRODUCTION

Retinal laser therapy, either alone or in combination with anti-VEGF agents or steroids, is widely used for the treatment of retinal disorders including proliferative diabetic retinopathy,[1] diabetic macular edema,[2] central serous retinopathy,[3] and retinal vein occlusions.[4] Since the introduction and establishment of laser photocoagulation as the standard of care in the early 1980's, several techniques to reduce overheating, and consequently damage, of the retina have been proposed. These include selective retinal therapy,[5] which injures only the retinal pigment epithelium (RPE) by using bursts of microsecond pulses to limit heat diffusion, sub-threshold diode micropulse,[6] which seeks a non-damaging endpoint with trains of microsecond pulses, sub-threshold transpupillary thermotherapy, which uses low power density over large laser spots and long pulses to target a non-damaging endpoint,[7–9] and non-damaging therapy using Endpoint Management (EpM), a titration algorithm based on lesion observation.[10] In clinical use, these treatments have been shown to be effective in treating chronic central serous retinopathy[11] and diabetic macular edema[6,12] while sparing the neural retina.

Ophthalmic Technologies XXVI, edited by Fabrice Manns, Per G. Söderberg, Arthur Ho, Proc. of SPIE Vol. 9693, 969319 · © 2016 SPIE · CCC code: 1605-7422/16/$18 · doi: 10.1117/12.2213171

Although clinical studies have demonstrated the effectiveness of non-damaging laser therapy, the mechanism of therapeutic effect remains unclear. While panretinal photocoagulation is believed to work in patients with proliferative diabetic retinopathy by killing a significant fraction of photoreceptors (about 30%) to reduce metabolic demands and inhibit angiogenesis, the mechanism leading to clinical benefits of the laser therapy in the macula was never clear. It has been noticed that non-damaging laser therapy is effective for macular disorders without destroying photoreceptors. One proposed mechanism of action is that laser-induced hyperthermia activates heat shock response in the RPE.[13] Heat shock proteins are known to act as chaperones for protein refolding, inhibit apoptosis, and downregulate inflammation.[14] The induction of these proteins, and activation of subsequent downstream repair pathways, is believed to rejuvenate RPE cells and improve their function.[15]

In this study, we use the EpM algorithm to apply a range of laser settings from non-damaging to conventional barely visible lesions in Dutch-belted rabbits. We use live/dead staining and histology to define the range of non-damaging parameters relative to the titration energy. Then, we measure the acute expression of 70 kDa heat shock protein (HSP70) by whole-mount immunohistochemistry to determine the window in which non-damaging laser treatment activates the heat shock response. We compare the areas of HSP expression in experiments with the computational model to better understand the optimal treatment parameters required for activating heat shock response in large areas of the retinal pigment epithelium.

2. MATERIALS AND METHODS

2.1 Laser system

A PASCAL Streamline 577 (Topcon Medical Laser Systems Inc., Santa Clara, CA) laser system was used to deliver 577 nm laser patterns to the retina. The beam profile is flat-top and a 200 μm diameter setting was used for all spots. To control for varying pigmentation, the threshold laser power needed to create barely visible lesions with 20 ms pulses when observed 3 s after laser delivery was set as the 100% energy point in each animal. For lower energy settings, the EpM titration algorithm previously described by Lavinsky et al.,[10] was used to decrease laser pulse duration and power for required tissue effect. Dash lines in Figure 1 show the laser settings corresponding to retinal lesions of various clinical grades characterized by the Arrhenius integral Ω. During titration with 20ms pulses, power was adjusted to produce a barely visible burn within 3 seconds of observation. The EpM algorithm (solid black line) adjusts the pulse duration and power such that 20% reduction in pulse energy corresponds to 10x steps in Ω. Tissue damage is expected at $\Omega > 1$ (area shown in red), and no tissue response below $\Omega < 0.1$ (area shown in blue).[16,17] The non-damaging treatment range (shown in green) corresponds to $1 < \Omega < 0.1$ For example, 30% pulse energy intersects the algorithm curve in the middle of the expected treatment range, while 40% energy point on the EpM curve is at the upper boundary of the damaging range.

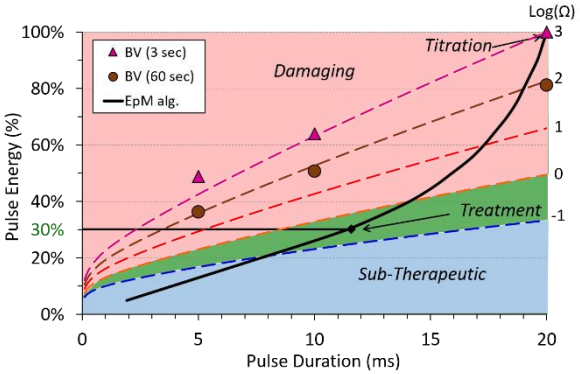

Figure 1. Endpoint Management (EpM) Algorithm. Dashed lines indicate curves of constant Arrhenius integral (Ω) with expected similar tissue effects. Barely visible (BV) when viewed 3 seconds after 20 ms laser pulse is used as the titration point. Solid black line shows laser pulse duration required for desired energy setting.

2.2 Laser application

A total of 15 Dutch-belted rabbits were used in accordance with the Association for Research in Vision and Ophthalmology Statement for the use of Animals in Ophthalmic and Visual Research, with approval from the Stanford University Animal Institutional Review Board. The rabbits were anesthetized with ketamine hydrochloride (35 mg/kg) and xylazine (5 mg/kg). Pupil dilation was achieved by 1 drop each of 1% tropicamide and 2.5% phenylephrine hydrochloride. Topical tetracaine hydrochloride (0.5%) was used for local anesthesia. A Mainster wide-field retinal contact lens (OMRA-WF, Ocular Instruments, Bellevue, WA) was used with hydroxypropyl methylcellulose as a contact gel. The conversion of aerial to retinal beam size with the contact lens on the rabbit eye was calculated to be 70% by comparing the pattern spacing between grids of lesions on the retina versus corresponding aerial patterns.

Treatment grids of 3x3 or 5x5 laser spots were applied with energies of 20%, 25%, 30%, 40%, 100% according to the EpM algorithm. Intense marker burns were applied to outline treatment areas and help locate non-damaging treatment patterns in subsequent analysis. Treatment was applied 7 hours before euthanasia for detection of acute HSP expression and viability staining. For histological analysis, animals were euthanized 1 day after laser treatment for best detection of structural changes.

2.3 Damage threshold determination

Immediately after euthanasia, the eye was enucleated, the anterior segment of the globe was removed, and the retina was manually peeled off of the RPE. For live/dead staining, the RPE-Choroid-Sclera sample was rinsed briefly in balanced salt solution (BSS) and then immersed in 2 μM Calcein AM/12 μM EthD-III (Viability/Cytotoxicity Assay, Biotium, Hayward, CA) solution for 30 minutes in a covered petri dish. Tissue samples were promptly imaged with fluorescence microscopy. For histology, the tissue was fixed in 1.25% glutaraldehyde/1% paraformaldehyde in cacodylate buffer, postfixed in osmium tetroxide, and dehydrated with a graded series of ethanol. The tissue was then processed with propylene oxide and embedded into epoxy resin (Embed 812; Electron Microscopy Sciences, Port Washington, PA). One-micrometer sections for light microscopy were cut on an ultramicrotome (Reichert-Jung Ultracut E; Leica, Deerfield, IL), stained with toluidine blue and photographed on a light microscope (Eclipse E1000; Nikon, Tokyo, Japan).

2.4 Immunohistochemistry

For whole-mount immunostaining of the RPE for HSP70 expression, the sclera, choroid and RPE were fixed in HistoChoice MB tissue fixative (Amresco LLC, Solon, OH) for 4 hours at room temperature. The tissue was then washed in phosphate buffered saline (PBS) and blocked for 1 hour at room temperature in PBS containing 5% normal goat serum. The tissue was incubated in 0.027 mg/mL mouse mAb anti-HSP70/72 (C92F3A-5, # ADI-SPA-810-F, ENZO Life Sciences, Farmingdale, NY) in PBS containing 1% normal goat serum at 4 oC overnight. This was followed by 3 x 15 minutes washes in PBS and incubation in PBS containing 0.027 mg/ml CF594 Goat anti-mouse IgG (H+L) secondary antibody (cat no. 20111, Biotium Inc., Hayward, CA) for 1 hour at room temperature. The tissue was then washed 3 x 15 minutes in PBS. The RPE and choroid were carefully separated from the sclera, mounted with glycerol mounting medium (ab188804, Abcam plc, Cambridge, UK), and imaged with a confocal microscope (Leica SP8 WLL, Leica Microsystems, Inc., Buffalo Grove, IL).

2.5 Computational Modeling

A finite-element model of 532 nm laser heating of the rabbit retina published by Sramek et al.[18] was adapted for 577 nm and used to predict temperature rise and tissue response using the Arrhenius damage integral. The adapted model, implemented with a computational package (COMSOL Multiphysics 5.0, Natick, MA), reduces the absorption coefficients

in the pigmented layers by 25% to account for lower 577 nm melanin absorption while increasing absorption coefficients in vascular layers by 25% to account for higher hemoglobin absorption.[19] To match the most common experimental titration value, the power at 100% energy setting was calculated with 70 mW power for 20 ms pulse and 140 μm beam, corresponding to the beam size on the rabbit retina. The Arrhenius damage integral is as follows:

$$\Omega(\tau) = A \int_0^{\tau} e^{-\frac{E^*}{R \cdot T(t)}} dt$$

where, T is the temperature, R is the gas constant, E* = 340 kJ/mol, A =1.55 X 10^{55} s^{-1}.[18] Previous studies[16],[17] showed that HSP expression and cell damage are expected to begin at Arrhenius values of $\Omega = 0.1$ and $\Omega = 1$, respectively. One unmeasured parameter, the ocular transmission of the laser delivery-eye system, was adjusted to 62% to match the observation that 30% energy setting is non-damaging ($\Omega \leq 1$).

3. RESULTS

3.1 Damage Threshold

Live/Dead (Biotium, Hayward, CA) staining was used to check for RPE damage after laser exposure. 4 eyes from 3 rabbits were treated with a total of 250 laser spots at 30% energy, 250 laser spots at 40% energy, and 54 laser spots at 100% energy. At 30% energy, none of the laser spots showed any dead cells. An example of the pattern area with no visible changes is shown in Figure 2a. At 40% energy, damage was visible in 69% of the delivered spots. Figure 2b presents one 5x5 40% pattern with dead RPE cells seen with EthD-III fluorescent red-stained nuclei. At 100% energy, all of the laser spots resulted in RPE cell death, as shown in Figure 2c demonstrating EthD-III stained nuclei as well as RPE cells that are missing entirely. The hazy red seen in several spots arises from out of focus staining of dead photoreceptors fused onto the RPE.

Histology was also used to analyze laser lesions at 20%, 30% and 70% energy setting. Laser was done 1 day before enucleation and the histology results are shown comparing undamaged 20% (Fig 3a) and 30% (Fig 3b) to damaged 70% area (Fig 3c). Neither 20% nor 30% area shows no structural indications of damage while 70% has outer segments fused to the RPE.

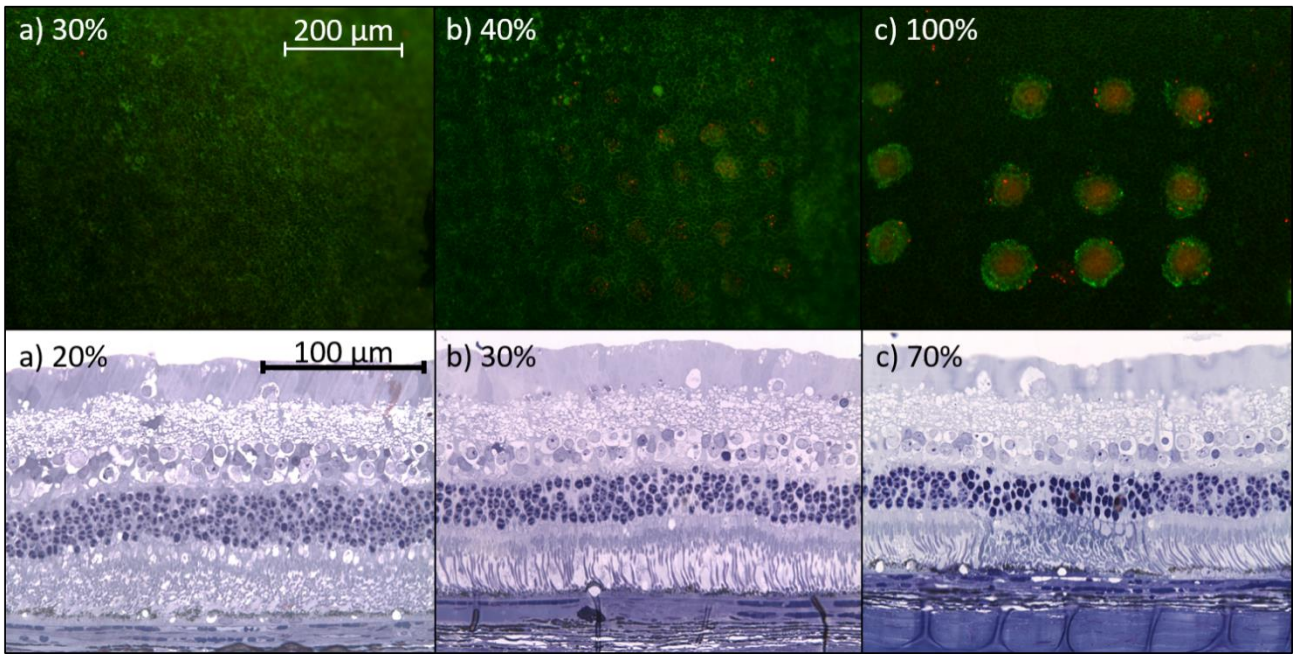

Figure 2. Damage threshold determination. Top row shows live/dead staining after laser treatment at given energy where green indicates live cells and red indicates dead cells. Bottom row shows toluidine blue stained sections.

3.2 Heat Shock Protein Expression

Confocal microscope images of immunostained RPE with laser patterns of 20%, 25%, 30%, 40%, and 100% energy were analyzed for expression of HSP70. No expression was observed at 20% energy with a total of 250 observed laser spots. For 25% energy (n = 200), 57% of laser spots showed HSP70 expression, while 30% energy (n = 238) and 40% energy (n = 150) had 98% and 99% expression, respectively. All laser spots at 100% (n = 54) showed HSP expression. Figure 3a-c shows patterns of 20%, 25% and 30% energy laser spots respectively. 20% shows no expression while 25% and 30% laser spots produce a disc of activated cells. In contrast, Figure 3d shows the 100% energy setting where expression occurs in a ring of cells.

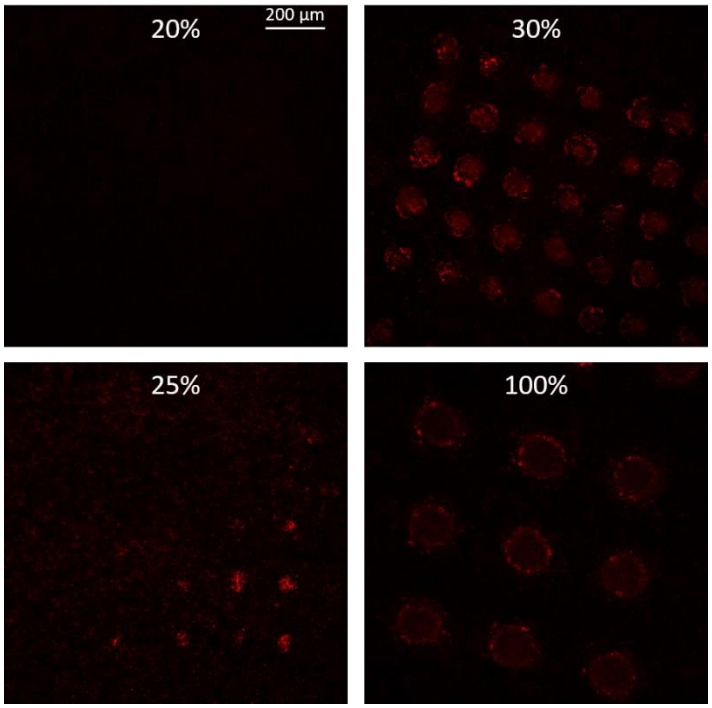

Figure 3. HSP70 expression on retinal pigment epithelium 7 hours after laser treatment

For each laser spot, the HSP expression area was measured. For 100%, the expression area was bounded by an inner and outer ellipse. Live/dead stained laser spots were similarly analyzed and the distribution of expression (left) or damage (right) diameters, the geometric mean of the major and minor axes, are shown in Figure 4.

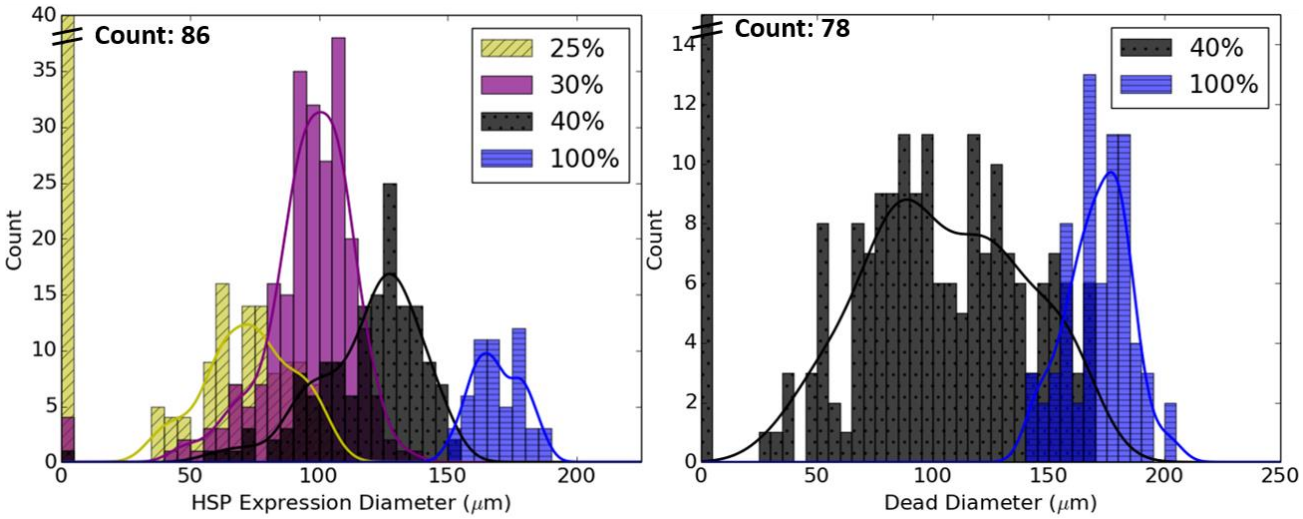

Figure 4. Histogram of HSP expression diameter and dead diameter. Overlayed curves show kernel density estimation fit for non-zero diameters.

3.3 Thermal Modeling

The computational model of laser heating was used to estimate the temperature rise during treatment. Figure 5 shows thermal maps of peak temperature rise for 30% and 100% settings. At 30%, the maximum temperature was calculated to be 66 °C, while barely visible lesions had peak temperatures up to 95 °C.

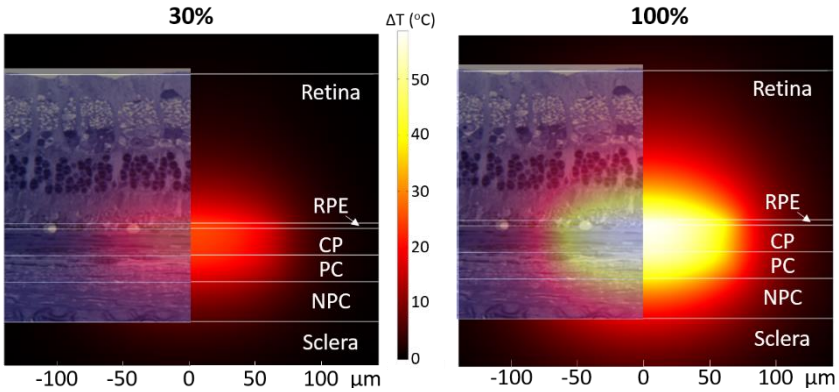

Figure 5. Thermal maps from computational model illustrating peak temperatures for 30% and 100% laser settings.

Arrhenius integrals were calculated from these temperature courses to predict damage area ($\Omega > 1$) and HSP70 expression area ($\Omega > 0.1$). These are shown for the experimentally measured settings in Figure 6 with the dotted lines outlining the areas of HSP expression and solid lines outlining areas of damage. The ring pattern of HSP expression at 100% settings can be explained by the fact that dead RPE cells don't express HSP, defining the upper bound of $\Omega < 1$ for HSP expression. Figure 7 shows the total expression area and total damage area per 100 laser spots as predicted by the model and as measured experimentally. The model predicts that expression area is maximized at the 40% setting with 0.73 mm^2 activated with 100 spots.

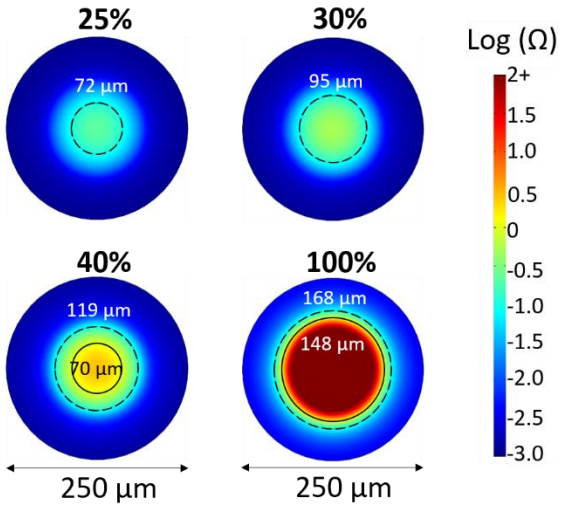

Figure 6. Arrhenius integral calculations for HSP expression and damage threshold. Dashed line indicates $\Omega = 0.1$ where HSP expression is expected to begin. Solid line indicates $\Omega = 1$ where cellular damage is expected.

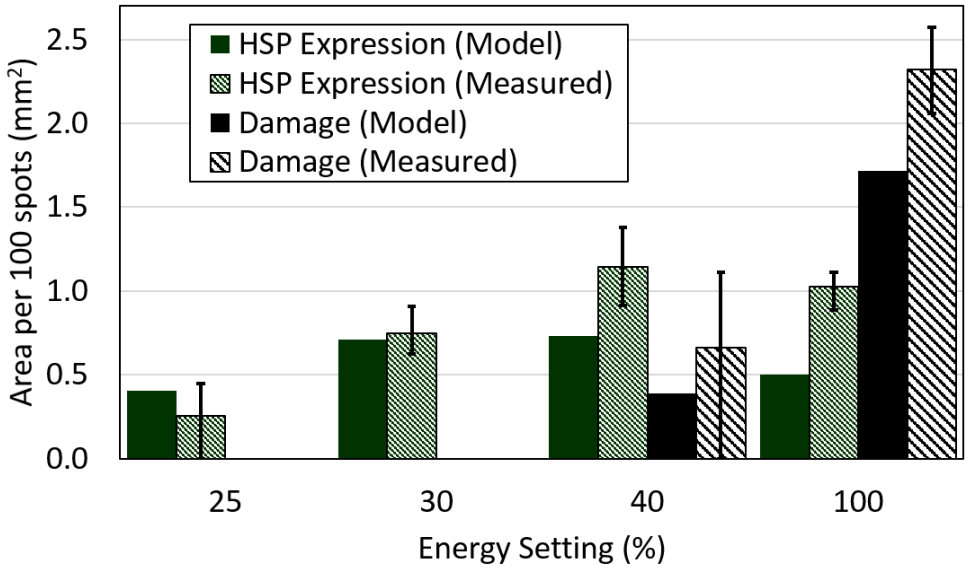

Figure 7. Expression and damage areas. Solid green and black bars show model predictions for area of HSP expression and damage respectively. Dashed green and black bars show experimental measurements of HSP expression and damage. Error bars give 1st and 3rd quartile values.

4. DISCUSSION

This study was performed to determine the threshold for safe, non-damaging therapy using the EpM titration system and to measure the tissue response to hyperthermia. Together, these establish the therapeutic window for non-damaging retinal laser therapy. Our results with live/dead staining showed that the damage threshold begins at 40% energy, matching the theoretical prediction shown in Figure 1. Across four eyes in 3 animals, 40% energy settings were damaging in 69% of the 250 total delivered spots. The distribution of damage diameters for 40% and 100% energy shown in Figure 4 shows the large range of tissue response, likely due to pigmentation fluctuation across the eye. Nonetheless, treatments at 30% energy were uniformly non-damaging following 250 experimental spots in 4 different eyes, suggesting that this setting is sufficiently below the damage threshold to account for normal pigment variation. Examination of histology from 30% laser spots also showed no damage, corroborating the live/dead staining results.

Tissue response to hyperthermia, measured by HSP expression in the RPE, begins at 25% setting. This is only slightly higher than the 20% value predicted by the theoretical model. HSP activation area increased with energy up to 40% (Figure 7), but at energies exceeding the damage threshold, the area of expression on the RPE became donut-shaped, with a dark center due to tissue damage, as shown for 100% settings in Figures 3 and 6. Only the cells at the "warm" edges of the hot laser spot survive the hyperthermia and express HSP. Therefore, increasing laser energy above the damage threshold is not expected to improve the therapeutic response from HSP activation. Instead, it just adds a damage zone in the center of the laser lesion. Activation area at 30% is a little smaller than the maximum response (at 40% and beyond), but lack of tissue damage allows application of much denser patterns which is likely to boost the therapeutic response.

Experimentally, the HSP expression area and the damage zone at 40% and 100% was larger than computed with the model (Figure 7) likely due to the cell size aliasing effect, where an entire RPE cell is activated or damaged, even if only a part of it falls in the HSP expression zone or damage zone. Given that the modelled expression zone at 100% is approximately 20 μm in width (Figure 6), and RPE cells are of a similar size, partial overlap of the cells with the activation area or damage zone would increase the observed expression area. Despite this discrepancy, the model is useful for understanding the activated HSP expression area and validating the EpM methodology.

Our results show that using EpM titration at 25-40% energy settings can induce HSP expression in the RPE without retinal damage. Although we've shown that heat shock proteins are expressed, the pathways leading to the therapeutic effects observed in treatment of chronic central serous retinopathy[11] and diabetic macular edema[6],[12] still need further study. Protein misfolding and aggregation in cell is a fundamental component of aging.[20] Normally, heat shock proteins refold the damaged proteins and thereby protects cells from protein aggregation and associated proteotoxicity.[21] However, transcriptional pathways decline in aging cells, leading to protein aggregation, commonly observed in neurodegenerative diseases.[22] Induction of HSP in aging cells helps maintaining the protein homeostasis by refolding damaged proteins, thereby promoting longevity and rejuvenating cellular functions. In addition, molecular chaperones, which include HSP27 and HSP70, have anti-apoptotic functions and therefore can prevent depletion of essential cell populations in degenerative processes.[23] Enhanced synthesis of HSP and co-chaperones in response to laser-induced thermal stress in RPE might normalize physiology of these cells in aging and disease.

5. CONCLUSIONS

Live/dead staining, histology, and whole-mount immunostaining of RPE in rabbits showed that laser treatment at 25-40% EpM settings can induce HSP expression without damage in the RPE. The expression window validates the predicted therapeutic window from the model and suggests a mechanism via endogenous repair pathways activated by hyperthermia. Non-damaging retinal laser therapy allows for treatment of the macula where damage, as seen in conventional photocoagulation, is prohibitive. Furthermore, application of high density patterns to increase therapeutic response and periodic retreatments for chronic retinal diseases are possible.

REFERENCES

[1] Group, T.D.R.S.R., "Photocoagulation Treatment of Proliferative Diabetic Retinopathy: Clinical Application of Diabetic Retinopathy Study (DRS) Findings, {DRS} Report Number 8," Ophthalmology 88(7), 583–600 (1981).

[2] ETDRS Study, "Photocoagulation for diabetic macular edema: Early treatment diabetic retinopathy study report number 1 early treatment diabetic retinopathy study research group," Archives of Ophthalmology 103(12), 1796–1806 (1985).

[3] Burumcek, E., Mudun, A., Karacorlu, S., and Arslan, M.O., "Laser photocoagulation for persistent central serous retinopathy: results of long-term follow-up.," Ophthalmology 104(4), 616–622 (1997).

[4] BVO Study Group, "Argon Laser Photocoagulation for macular edema in branch vein occlusion," American Journal of Ophthalmology 98(3), 271–282 (1984).

[5] Roider, J., Hillenkamp, F., Flotte, T., and Birngruber, R., "Microphotocoagulation: selective effects of repetitive

short laser pulses.," Proceedings of the National Academy of Sciences of the United States of America 90(18), 8643–8647 (1993).

[6] Luttrull, J.K., Musch, D.C., and Mainster, M.A., "Subthreshold diode micropulse photocoagulation for the treatment of clinically significant diabetic macular oedema.," The British journal of ophthalmology 89(1), 74–80 (2005).

[7] Journée-De Korver, J.G., Oosterhuis, J.A., Kakebeeke-Kemme, H.M., and de Wolff-Rouendaal, D., "Transpupillary thermotherapy (TTT) by infrared irradiation of choroidal melanoma," Documenta Ophthalmologica 82(3), 185–191 (1992).

[8] Mainster, M.A., and Reichel, E., "Transpupillary thermotherapy for age-related macular degeneration: long-pulse photocoagulation, apoptosis, and heat shock proteins," Ophthalmic surgery and lasers 31(5), 359 (2000).

[9] Fuisting, B., and Richard, G., "Transpupillary thermotherapy (TTT) – Review of the clinical indication spectrum," Medical Laser Application 25(4), 214–222 (2010).

[10] Lavinsky, D., Sramek, C., Wang, J., Huie, P., Dalal, R., Mandel, Y., and Palanker, D., "Subvisible retinal laser therapy: titration algorithm and tissue response.," Retina 34(1), 87–97 (2014).

[11] Lavinsky, D., and Palanker, D., "NONDAMAGING PHOTOTHERMAL THERAPY FOR THE RETINA," Retina 35(2), 213–222 (2015).

[12] Lavinsky, D., Cardillo, J.A., Melo, L.A.S., Dare, A., Farah, M.E., and Belfort, R., "Randomized clinical trial evaluating mETDRS versus normal or high-density micropulse photocoagulation for diabetic macular edema," Investigative Ophthalmology and Visual Science 52(7), 4314–4323 (2011).

[13] Sramek, C., Mackanos, M., Spitler, R., Leung, L.-S., Nomoto, H., Contag, C.H., and Palanker, D., "Non-damaging Retinal Phototherapy: Dynamic Range of Heat Shock Protein Expression," Investigative Opthalmology & Visual Science 52(3), 1780 (2011).

[14] Yenari, M.A., Liu, J., Zheng, Z., Vexler, Z.S., Lee, J.E., and Giffard, R.G., "Antiapoptotic and anti-inflammatory mechanisms of heat-shock protein protection," Annals of the New York Academy of Sciences 1053(127), 74–83 (2005).

[15] Luttrull, J.K., Chang, D.B., Margolis, B.W.L., Dorin, G., and Luttrull, D.K., "LASER RESENSITIZATION OF MEDICALLY UNRESPONSIVE NEOVASCULAR AGE-RELATED MACULAR DEGENERATION," Retina 35(6), 1184–1194 (2015).

[16] Sramek, C., Mackanos, M., Spitler, R., Leung, L.-S., Nomoto, H., Contag, C.H., and Palanker, D., "Non-damaging retinal phototherapy: dynamic range of heat shock protein expression," Investigative ophthalmology & visual science 52(3), 1780–7 (2011).

[17] Luttrull, J.K., Sramek, C., Palanker, D., Spink, C.J., and Musch, D.C., "LONG-TERM SAFETY, HIGH-RESOLUTION IMAGING, AND TISSUE TEMPERATURE MODELING OF SUBVISIBLE DIODE MICROPULSE PHOTOCOAGULATION FOR RETINOVASCULAR MACULAR EDEMA," Retina 32(2), 375–386 (2012).

[18] Sramek, C., Paulus, Y., Nomoto, H., Huie, P., Brown, J., and Palanker, D., "Dynamics of retinal photocoagulation and rupture.," Journal of biomedical optics 14(3), 034007 (2009).

[19] Sramek, C.K., Leung, L.-S.B., Paulus, Y.M., and Palanker, D. V., "Therapeutic Window of Retinal Photocoagulation With Green (532-nm) and Yellow (577-nm) Lasers," Ophthalmic Surgery Lasers Imaging 43(4), 341–347 (2012).

[20] Murshid, A., Eguchi, T., and Calderwood, S.K., "Stress proteins in aging and life span," International Journal of Hyperthermia 29(5), 442–447 (2013).

[21] Sreekumar, P.G., Kannan, R., Kitamura, M., Spee, C., Barron, E., Ryan, S.J., and Hinton, D.R., "αB crystallin is apically secreted within exosomes by polarized human retinal pigment epithelium and provides neuroprotection to

adjacent cells," PLoS ONE 5(10), e12578 (2010).

[22] Gestwicki, J.E., and Garza, D., [Protein quality control in neurodegenerative disease] , 1st ed., in Prog. Mol. Biol. Transl. Sci. 107, 1st ed., Elsevier Inc. (2012).

[23] Chopek, J.W., and Gardiner, P.F., "Life-long caloric restriction: Effect on age-related changes in motoneuron numbers, sizes and apoptotic markers.," Mechanisms of ageing and development 131(10), 650–9 (2010).